Biogeosciences, 8, 1853–1863, 2011
www.biogeosciences.net/8/1853/2011/
doi:10.5194/bg-8-1853-2011

Biogeosciences

Vertical and longitudinal gradients in HNA-LNA cell abundances and cytometric characteristics in the Mediterranean Sea

F. Van Wambeke[1], **P. Catala**[2,3], **M. Pujo-Pay**[2,3], **and P. Lebaron**[2,3]

[1]CNRS, Université de la Méditerranée, Laboratoire de Microbiologie, Géochimie et Ecologie Marines, UMR6117, Case 901, Campus de Luminy, 13 288 Marseille cedex 9, France
[2]UPMC Univ Paris 06, Laboratoire ARAGO – Observatoire Océanologique, 66651 Banyuls/mer, France
[3]CNRS, UMR7621, LOMIC, Observatoire Océanologique, 66651 Banyuls/mer, France

Received: 29 October 2010 – Published in Biogeosciences Discuss.: 10 November 2010
Revised: 18 June 2011 – Accepted: 20 June 2011 – Published: 13 July 2011

Abstract. Heterotrophic bacterioplankton abundance and production were investigated with depth (down to bathypelagic layers) and with longitude (from 4.9° E to 32.7° E) along a cruise track across the Mediterranean Sea in early summer 2008. Abundances and flow cytometric characteristics (green fluorescence and side scatter signals) of high nucleic acid (HNA) and low nucleic acid (LNA) bacterial cells were determined using flow cytometry. Contrary to what is generally observed, the relative importance of HNA cells, as a percent of total cells, (%HNA, range 30–69 %) was inversely related to bacterial production (range 0.15–44 ng C l^{-1} h^{-1}) although the negative relation was weak (log–log regression $r^2 = 0.19$). The %HNA as well as the mean side scatter of HNA group increased significantly with depth in the meso and bathypelagic layers. Vertical stratification played an important role in influencing the distribution and characteristics of bacterial cells especially with regard to layers located above, within or below the deep chlorophyll maximum. Within a given layer, the relationships between the flow cytometric characteristics and environmental variables such as chlorophyll-*a*, nutrients or bacterial production changed. Overall, the relationships between HNA and LNA cells and environmental parameters differed vertically more than longitudinally.

1 Introduction

Flow cytometry is a powerful tool to study microbial communities. In samples from aquatic environments, bacterioplankton cells tend to cluster into at least 2 or 3 distinct fractions based on differences in the side scatter signal (SSC, related to the size, density and morphology of the cells) and in the relative green fluorescence (related to the nucleic acid content of the cells). These fractions are more generally named HNA (high nucleic acid) and LNA (low nucleic acid) cells (Lebaron et al., 2001). Many papers have reported abundances of HNA and LNA cells over a wide range of environmental samples, from oligotrophic to eutrophic environments, since the pioneering work of Li et al. (1995). However, factors influencing the relative importance of HNA to LNA cells both within and among aquatic systems are unclear. Comparisons among studies are hindered as different protocols are used (differences in instrument, sample fixation and storage, nucleic acid stain, etc.). Thus, comparisons have generally been made on population abundance, and few have considered cytometric characteristics.

Within systems, a variety of patterns have been reported. Corzo et al. (2005) examined distributions with depth through a 0–100 m water column in the Drake Passage and Gerlache Straits during the austral summer. SSC and green fluorescence of HNA cells were closely related to chlorophyll-*a* whereas those of LNA cells were not. In contrast, Sherr et al. (2006) showed that the ratios HNA/LNA for abundance and green fluorescence were remarkably stable along large inshore-offshore gradients in the northeast Pacific Ocean, concluding that HNA cells were not more responsive than LNA cells to chlorophyll variability. When examined over a broad range of trophic conditions (bacterial production covering 4 orders of magnitude, from 0.01 to 11.6 µg C l^{-1} h^{-1} and chlorophyll-*a* 0.2 to 69 µg l^{-1}), cytometric characteristics changed greatly in different ecosystems and along productivity gradients (Bouvier et al., 2007). The patterns did not support the simple, dichotomous view of HNA and LNA bacteria as active and inactive cells, as

Correspondence to: F. Van Wambeke
(france.van-wambeke@univmed.fr)

hypothesized by early cell sorting experiments (Servais et al., 1999; Lebaron et al., 2001). The general conclusion from the literature is that HNA bacteria are larger and more active on a cell basis than LNA bacteria. Overall, despite considerable amount of work, the contribution of LNA cells to total bacterial production is still a subject of much debate (Longnecker et al., 2006; Sherr et al., 2006; Scharek and Latasa, 2007; Moran et al., 2010).

The Mediterranean Sea is largely oligotrophic over much of the year, and is characterized by a gradient of oligotrophy from the oligotrophic West to the ultra-oligotrophic East. The BOUM (Biogeochemistry from the Oligotrophic to the Ultra-oligotrophic Mediterranean) cruise carried out in early summer 2008, offered the opportunity to examine bacterial abundance and production with depth over a large longitudinal gradient. Indeed, to our knowledge, information available in Mediterranean Sea about HNA and LNA cytometric group distributions and properties is restricted to Western, coastal and shelf areas (Lebaron et al., 2001; Joux et al., 2005; Scharek and Latasa, 2007). Very limited data on LNA and HNA distributions within open sea areas are available: the Dyfamed site in the N.W. Mediterranean has been studied on different time scales but with no reports on variability of cytometric properties like SSC or fluorescence (Mével et al., 2008; Winter et al., 2009).

In this study we analyzed a large number of samples to investigate flow cytometric characteristics in relation to bacterial production and environmental parameters (temperature, total chlorophyll-*a*, phosphate, nitrate + nitrite). Samples were gathered from surface to mesopelagic waters from 30 stations across the Mediterranean Sea. The aim of this study was to explore the factors that determine the variability in abundances and cytometric properties of HNA and LNA cells in Mediterranean Sea waters, including the deep sea and the Eastern Basin. Flow cytometric characteristics of the bacterioplankton were examined within layers located above, within and below the deep chlorophyll maximum, as well as longitudinally among different regions.

2 Material and methods

2.1 Study area and sample collection

This work was carried out during the "BOUM" cruise on the R/V *Atalante* during June–July 2008. The cruise was planned as a transect of stations encompassing a large longitudinal gradient in the Mediterranean Sea (Fig. 1). Samples were collected using a rosette of 24 × 12 l Niskin bottles mounted on a CTD rosette system. Sensors on the CTD provided profiles for temperature, salinity, and fluorescence at each station. The depth of the deep chlorophyll maximum (dcm) was determined from the fluorescence profile. Total chlorophyll-*a* (TChl-*a*) was analyzed using HPLC (Ras et al., 2008) and the data for vertical and horizontal

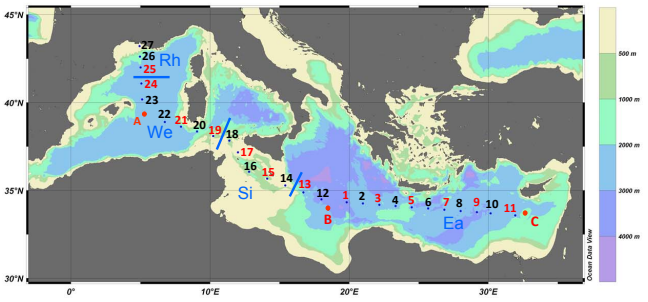

Fig. 1. Map of the BOUM transect. All stations were sampled for bacterial abundances and TChl-*a* whereas only stations indicated with a code in red were sampled for bacterial production. Blues characters and lines separates the different regions compared (see Material and Method section). Figures 1 and 3 were drawn with Ocean Data View program (Schlitzer, 2009).

profiles are presented in Moutin et al. (2011) and Crombet et al. (2011). Phosphate (PO_4^{3-}) and nitrate + nitrite (NO_3^- + NO_2^-) were analysed using automated colorimetric technique as described in Pujo-Pay et al. (2011). Detection limits for the procedures were 0.01 µM for PO_4^{3-} and 0.02 µM for NO_3^- + NO_2^-. The numbered stations were occupied briefly and sampled at different times of the day. All these numbered stations were investigated for bacterial abundance and only one half of them for bacterial production (1, 3, 5, 7, 9, 11, 13, 15, 17, 19, 21, 24, 25). Sites designated by letters (A, B and C) were gyre stations, located inside anticyclonic gyres and each was sampled over a 4 day period. At each gyre station, up to 4 depth profiles for bacterial abundance and production were obtained, three at 09:00 a.m., and one at 02:00 a.m. (local time). The whole data set was used to describe bacterial abundance over 45 vertical profiles (493 samples) while relationships with BP were examined using 25 profiles (198 samples).

2.2 Flow cytometric analysis of bacteria

Aliquots of 1.8 ml were taken for heterotrophic bacterioplankton (sensus stricto referring to heterotrophic prokaryotes), fixed with 2 % (w/v) formaldehyde (PFA) solution, stored for at least 30 min at room temperature, frozen in liquid nitrogen and then stored at −80 °C until samples could be processed on shore.

Samples were left to thaw at room temperature and stained with SYBR Green I (Invitrogen–Molecular Probes) at 0.025 % (vol/vol) final concentration for 15 min at room temperature in the dark. Counts were performed using the FacsCalibur flow cytometer (Becton Dickinson) equipped with an air-cooled argon laser (488 nm, 15 mW). The sheath fluid was filtered (< 0.2 µm) seawater. Stained bacterial cells, excited at 488 nm, were discriminated and enumerated according to their right-angle light scatter (SSC, related to cell size) and green fluorescence (530/30 nm). The speed

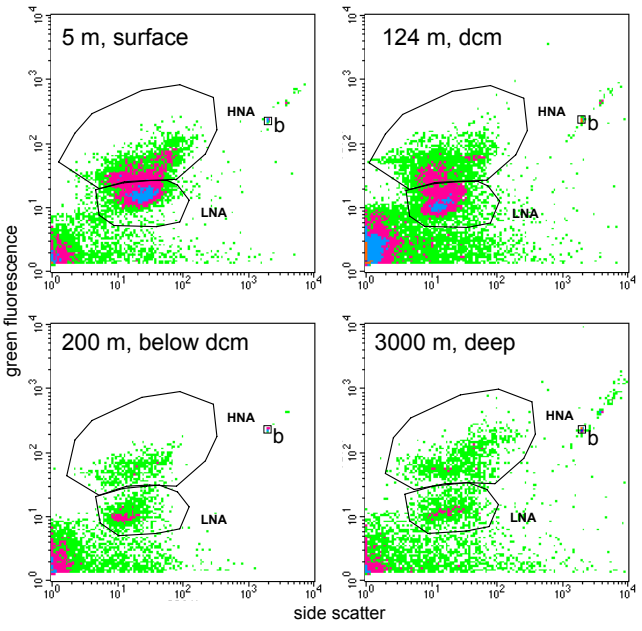

Fig. 2. Examples of four cytograms obtained after SyBR green I staining. The data comes from Station B (Ionian Sea): surface (5 m), at the dcm (125 m), below dcm (200 m) and in deep layers (3000 m). Time of analysis was set to 1 min for the 3 first layers, and 3 min for the 3000 m layer. Windows for HNA and LNA cells are drawn and were adjusted from one sample to another. b: 1 µm beads.

of the analysis was dependant on the bacterial abundance of the sample, typically the volume analyzed was around 20 µl (low speed). The subsequent cell concentration estimation was determined from the flow rate, which was calculated by weighing one tube of milliQ water before and after a 5 min run of the cytometer (this flow rate calibration was done after each five sample tubes). Fluorescent beads (1.002 µm, Polysciences Europe) were systematically added to each sample as an internal standard and used to normalize values of single cell variables. Thus, the fluorescence and side scatter values of cells were standardized to those of the reference beads to account for potential differences in measurement conditions (all samples were analysed during a 6 month-period by the same analyst). In a plot of green fluorescence versus red fluorescence we were able to distinguish photosynthetic prokaryotes which were removed from non-photosynthetic prokaryotes. Bacteria with a high nucleic acid content (HNA cells) were discriminated from bacteria with a low nucleic acid content (LNA cells). Each subgroup was delimited on the SSC versus green fluorescence plot by drawing a gate, and cell abundance was determined in each subgroup (Fig. 2). Windows were adjusted for each individual sample. Total abundance is determined as LNA + HNA and the percentage of HNA cell abundance (%HNA) was calculated as HNA/(HNA + LNA).

2.3 Bacterial production

"Bacterial" production (BP – sensus stricto referring to heterotrophic prokaryotic production –) was determined by [^{3}H] leucine incorporation applying the centrifugation method (Smith and Azam, 1992). Duplicate 1.5 mL samples and one trichloracetic acid (TCA) killed control for blank correction were incubated with a mixture of [4,5–^{3}H]leucine (Perkin Elmer, specific activity 115 Ci mmol^{-1}) and nonradioactive leucine at final concentrations of 16 and 7 nM, respectively. Samples were incubated in the dark at the respective in situ temperatures for 2–5 h depending on the expected activity. Preliminary checks showed that the incorporation of leucine was linear with time. Incubations were stopped by adding of TCA to a final concentration of 5 %. To facilitate the precipitation of proteins, bovine serum albumin (BSA, Sigma, 100 mg L^{-1} final concentration) was added prior to centrifugation which was carried out at 16 000 g for 10 min. After discarding the supernatant, 1.5 ml of 5 % TCA was added and the samples were vigorously shaken using a vortex and then centrifuged again. After discarding the supernatant, 1.5 ml of 80 % ethanol was added and then the samples were shaken and centrifuged again. The supernatant was discarded, and 1.5 ml Ultimagold MW added in the centrifuge tube. The radioactivity incorporated into the pellet was counted using a Packard LS 1600 Liquid Scintillation Counter. A factor of 1.5 kg C mol leucine^{-1} was used to convert the incorporation of leucine to carbon equivalents, assuming no isotopic dilution. This was checked on 3 occasions with concentration kinetics (range of concentrations 3 to 50 nM, isotopic dilution between 1.01 and 1.07). Activities within meso- and bathy-pelagic layers were also investigated at stations A, B and C, between 250 and 910 m at St C, 250–3000 m at St B and 250–2700 m at St A. These deeper samples, where a lower activity was expected, were treated by the filtration technique (Kirchman, 1993). We added 10 nM final concentration of [4,5–^{3}H]leucine in 50 ml samples. Two duplicates and one formalin-killed blank were incubated in the dark at in situ temperature for 15–20 h. Live samples were terminated by formalin addition (1 % final concentration) and all samples were filtered onto 0.2 µm Millipore GS/WP filters before TCA extraction (5 % final) and a 80 % ethanol rinse directly on the filter tower. Filters were dissolved in 1 ml of ethyl acetate before addition of Ultima Gold MV scintillation cocktail. Errors associated with the variability between replicate measurements (half the difference between the two replicates) averaged 6 % and 8 % for BP values determined using the centrifuge (surface samples) and filtration (deep samples) methods, respectively.

2.4 Statistical analysis and groups of data

For comparison of each parameter between different regions or vertical layers, statistical analysis was done by post hoc Fisher PLSD test after an ANOVA test. Abundance variables

and cytometric characteristics as well as BP and environmental parameters (temperature, chlorophyll, nutrients) were $\log_{10}$ transformed in order to achieve normality and homogeneity of variances before making correlations or ANOVA. Respecting recommendations of Sokal and Rohlf (1981), data sets including values between zero and one were multiplied by 100 (green fluorescence) or 1000 (SSC) before log transformation to avoid negative characteristics in the logarithms. PO_4^{3-} and NO_3^- + NO_2^- data sets also included many zeros and their transformation was done applying the formula LOG(data*100 + 1). Model II regression was used to examine relationships between 2 parameters when both (used in X and Y axis) were subjected to measurement variability. Model I was used to examine the relationship between any Y environmental dependant variable and an X independent variable as temperature or depth. Note that the coefficient of determination is the same whatever the model used.

Relationships were examined vertically following 4 different groups of samples:

- "surface" samples located between the surface and the deep chlorophyll maximum (dcm) layer,
- "dcm" samples at the dcm depth,
- "below dcm" corresponds to samples taken between the dcm and 250 m,
- "deep" corresponds to samples taken below 250 m.

Indeed, the "dcm" layer represents an ideal ecological boundary in our study which enabled data to be compared from stations across the Mediterranean Sea, where the transparency of water, depths of nutriclines and dcm varied greatly (Pujo Pay et al., 2011; Crombet et al., 2011).

Longitudinally, we compared 4 groups defined as follows: (i) "Rh" including North Western Mediterranean Sea stations (25 to 27) which were closer to the Rhône river with a higher chlorophyll biomass and bacterial abundances and a chlorophyll maximum between 3 and 50 m; (ii) "We" including stations 19 to 24 and A located in open Western Mediterranean with deeper dcm depths (between 69 and 96 m); (iii) "St" with stations 14 to 17 (within the Sicily strait) and station 18 which is in the Western basin but its intermediary layers are influenced by the flow of subsurface Eastern waters (Pujo-Pay et al., 2011); and (iv) "Ea" including stations 1 to 13 and stations B and C located in open, Eastern Mediterranean (Fig. 1).

3 Results

3.1 Distribution and variability of biological and physico-chemical parameters

The stations were located between 43.2° N, 4.93° E (close to Rhône river mouth) and 33.7° N, 32.7° E (South of Cyprus,

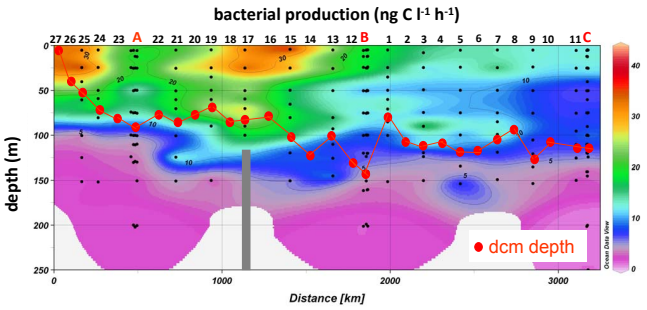

Fig. 3. Contour plot of bacterial production along the BOUM transect, from the most Northwestern station (left) to the most Eastern station (right) and for the 0–250 m layer. Depth of the deep chlorophyll maximum (dcm) is also indicated (red dots). The bar at St 7 in the Sicily strait shows the bottom depth (116 m).

on the sea mount Erathostène, Fig. 1). All stations were situated within the continental slope or open Sea (except at the Sicily Strait: St 14, 382 m and St 17, 116 m and close to the Rhone river mouth: St 27, 105 m), with bottom depths down to 3321 m (st 12). The diel variability of sea surface temperature per station was around 1 °C. Surface temperature (5 m) reached a maximum of 27.5 °C (st 12 in the Levantine Sea) with lowest temperatures at St 27 (17.2 °C, close to the Rhône river mouth) and decreasing with depth down to 13.3 °C in the Eastern Basin and 12.8 °C in the Western Basin (Table 1).

There was a classical West – East gradient of the deepening of the depth of the dcm (Fig. 3), which varied from 5 m at the western station 27 to 145 m at eastern station B. Maximum TChl-*a* concentration was found at station 25, with 1.7 µg TChl-*a* l^{-1} at 50 m depth. Based on integrated TChl-*a* (concentrations measured down to 250 m), the most oligotrophic station was station 8, with 16.1 mg TChl-*a* m^{-2} whereas the richest was station 25 (55.3 mg TChl-*a* m^{-2}).

"Surface layers" were low in PO_4^{3-} and in NO_3^- + NO_2^- throughout the transect (see Fig. 3 in Pujo-Pay et al., 2011), although at some stations (st C in Levantine Basin, St 19, 20, 21, 22, and 27 in the Western Basin), PO_4^{3-} values were slightly above the detection limit. PO_4^{3-} decreased significantly in the "surface layers" from the region West ("We": 0.012 ± 0.013 µM) to region East ("Ea": 0.008 ± 0.014 µM, $p = 0.02$) as well as in "below dcm" layers ("We": 0.16 ± 0.10 µM, "Ea": 0.04 ± 0.04 µM, $p < 0.001$); and in the "deeper layers" ("We": 0.35 ± 0.03 µM, "Ea": 0.15 ± 0.05 µM, $p < 0.001$). There was no statistical difference in the mean PO_4^{3-} concentration in the "dcm" layer among regions. The means of NO_3^- + NO_2^- did not change significantly among the different basins for "surface" and "dcm" layers, but significantly decreased in "below dcm" layers from "We" (4.8 ± 2.7 µM) to "Ea" (2.0 ± 1.4 µM) regions. Significant changes in the means between Eastern and Western Basins within the "below dcm layers" were mainly

Table 1. Ranges of salinity, temperature, total chlorophyll-*a* (TChl-*a*), phosphate (PO_4^{3-}), nitrate + nitrite (NO_3^- + NO_2^-), total bacterial abundance (total ab), and bacterial production (BP) for the data set used for comparison of abundance and cytometric characteristics of HNA and LNA cells. Means, coefficient of variation and number of data for each group of water column partition: layers above the deep chlorophyll maximum (surface), layers at the deep chlorophyll maximum ("dcm"), layers below the dcm but above or equal to 250 m ("below dcm"), and layers below 250 m "deep". bdl: below detection limits.

	Salinity PSU	temperature °C	TChl-*a* µg l^{-1}	PO_4^{3-} µM	NO_3^- + NO_2^- µM	total ab × 10^5 ml^{-1}	BP ng C l^{-1} h^{-1}
N	493	493	296	417	417	493	198
min	37.24	12.9	0.0004	bdl	bdl	0.15	0.15
max	39.65	27.5	1.7	0.393	9.81	13.40	43.9
surface	38.33	19.7	0.098	0.008	0.040	4.62	15.0
	(1.8 %, $n = 192$)	(18 %, $n = 192$)	(74 %, $n = 111$)	(155 %, $n = 148$)	(392 %, $n = 148$)	(33 %, $n = 192$)	(60 %, $n = 110$)
dcm	38.42	15.8	0.43	0.015	0.46	5.18	15.2
	(1.6 %, $n = 45$)	(7 %, $n = 45$)	(67 %, $n = 30$)	(112 %, $n = 38$)	(130 %, $n = 38$)	(43 %, $n = 45$)	(61 %, $n = 24$)
below dcm	38.60	14.9	0.059	0.101	3.46	2.36	3.62
	(1.2 %, $n = 201$)	(8 %, $n = 201$)	(137 %; $n = 154$)	(98 %, $n = 175$)	(79 %, $n = 175$)	(49 %, $n = 201$)	(96 %, $n = 54$)
deep	38.63	13.4		0.277	7.50	0.53	0.48
	(0.4 %, $n = 55$)	(5 %, $n = 55$)		(35 %, $n = 55$)	(28 %, $n = 55$)	(110 %, $n = 55$)	(123 %, $n = 10$)

due to the deepening of nutriclines in the East, and for "deep" layers were due to the different origin of deep waters masses in Eastern and Western Basins (see Pujo-Pay et al., 2011).

3.2 Total bacterial abundance and production

Total bacterial abundances ranged from 0.15 to 13.4×10^5 ml^{-1} (Table 1). BP ranged from 0.1 ng C l^{-1} h^{-1} (650 m, station C) to 43.9 ng C l^{-1} h^{-1} (Sicily Strait, 5 m, station 15), and 41 ng C l^{-1} h^{-1} at the station sampled for BP closest to the Rhône river mouth (25 m, station 25, Fig. 3).

The relationship between bacterial biomass (BB, calculated assuming 12 fgC per cell) and BP was high ($r^2 = 0.7$) when the data were pooled all together (data not shown). r^2 was lower but remained significant for different layers ($r^2 = 0.24$, 0.54 and 0.47 for "surface", "dcm" and "below dcm" layers, respectively). The slopes obtained for the whole data set (0.57) as well as for the separate water-column layers (0.44–0.55) suggest bottom-up control of bacterial biomass following Billen et al. (1990) and Ducklow (1992). TChl-*a* was weakly linked to BP (29 % of the variability explained, relation not shown). Notably in different layers, there was no relationship between TChl-*a* and BP for "surface" layers, and weak relationships for the "dcm" and "below dcm" layers ($r^2 = 0.52$ and 0.53). There was not any relationship between BP and concentration of PO_4^{3-} (log transformed data, $p > 0.05$) regardless of layer.

3.3 HNA and LNA bacterial abundance

All samples had two HNA and LNA cell fractions discernable by fluorescence versus SSC cytograms. HNA cell abundances ranged from 7.7×10^3 to 6.1×10^5 ml^{-1}, and those of LNA cells from 6.5×10^3 to 7.3×10^5 ml^{-1}. Both box-plot distributions of HNA and LNA cells showed high variability within the "surface" and "dcm" layers (Fig. 4a, b). Neither HNA nor LNA cell abundances were statistically different in the "surface" when compared to the "dcm" layers (ANOVA, threshold chosen at $p = 0.01$), but significantly decreased "below the dcm" and in the "deep" layers (ANOVA, $p < 0.01$). The decrease in HNA and LNA cell abundances with depth (log-log regressions abundance-depth) were significant for "dcm", "below dcm" and "deep" layers (r^2 ranged 0.33–0.66, for all regressions $p < 0.01$). Surprisingly, the percentage of HNA cell abundance (%HNA = HNA/(LNA + HNA)) increased significantly with depth in the meso- and bathypelagic zones (log-log regression in the "deep" layers, $r^2 = 0.59$, $n = 55$, Fig. 5b), whereas for the other layers the correlation was insignificant.

Longitudinal variability was examined in the different vertical layers. Within the "surface" layer a West- East gradient was visible for both HNA and LNA abundances, with significantly higher values in the "Rh" region and lower values in "Ea" compared to "We" region (Fig. 6a, b). However, these differences in abundances among different regions were concomitant for both groups as longitudinally, %HNA did not change (see for example %HNA distribution in "surface layers" Fig. 7a).

BP was responsible for 65 % and 70 % of the variability in HNA and LNA cell abundance, respectively, but the positive slope of the log-log regression was higher for the LNA cells (0.62 versus 0.53, with model II, figure not shown). Consequently, %HNA decreased slightly with increasing BP (the log-log regression was barely significant, $r^2 = 0.19$, Fig. 8). However, the log-log relation between %HNA and BP was insignificant for "surface", "below dcm" and "deep" layers, but BP explained (with a positive slope) 21 % of the variability of %HNA in the "dcm" layers (Table 2).

Table 2. Relationships between abundance of HNA cells, abundance of LNA cells and %HNA versus TChl-*a*, versus BP, versus soluble reactive phosphorus (PO_4^{3-}) and versus nitrate + nitrite (NO_3^- + NO_2^-) concentrations. Data were transformed before fitting with linear regressions (see methods). n: number of data, r^2: determination coefficient, nd: not determined, ns: not significant (Significant threshold set at $p = 0.05$). For clarity, sign of slopes for weak correlations ($r^2 < 0.1$) were not indicated. The number of data used in the regressions for each type of environmental variable and for each layer are indicated in Table 1.

		relation with Tchl-*a*		relation with BP		relation with PO_4^{3-}		realtion with NO_3^- + NO_2^-	
		Sign of slope	r^2	sign of slope	r^2	sign of slope	r^2	sign of slope	r^2
HNA	all data	+	0.59	+	0.65	–	0.46	–	0.41
abundance	surface	+	0.32	+	0.25		ns		ns
	dcm	+	0.41	+	0.52		ns		ns
	below dcm	+	0.55	+	0.42		0.08	–	0.19
	deep		nd		ns		ns		ns
LNA	all data	+	0.6	+	0.70	–	0.49	–	0.46
abundance	surface	+	0.26	+	0.21		ns		ns
	dcm	+	0.4	+	0.49		ns		ns
	below dcm	+	0.64	+	0.46		0.07	–	0.16
	deep		nd		ns		ns		ns
%HNA	all data		0.07	–	0.19	+	0.21	+	0.24
	surface		ns		ns		ns		ns
	dcm	+	0.12	+	0.21		ns		ns
	below dcm		0.02		ns		ns		ns
	deep		nd		ns		ns		ns

TChl-*a* appeared to explain a large variability in cell abundances. Both HNA and LNA cell abundances showed a significant, positive slope following TChl-*a* concentrations (slopes model II: 0.31, $r^2 = 0.59$; 0.34, $r^2 = 0.60$, respectively). The correlations of abundances with Tchl-*a* were also significant within the 3 chlorophyll layers when considered independently ("surface", "dcm" and "above dcm"). TChl-*a* explained slightly the variability of %HNA only at the "dcm" layer ($r^2 = 0.12$, Table 2).

Abundances of HNA and LNA were also inversely related to concentrations of phosphate and nitrate + nitrite (r^2 ranged 0.41 to 0.49, Table 2). Some of the %HNA variability was explained by variability of PO_4^{3-} ($r^2 = 0.21$) and NO_3^- + NO_2^- ($r^2 = 0.24$). Such relationships were mainly due to the co-variation with depth as this relationship weakened and/or disappeared when layers were considered separately (Table 2).

Finally, plotting the data all together ("surface", "dcm", "below dcm" and "deep") the log-log relationship between %HNA , LNA cell abundances and HNA cell abundances with temperature was weakly significant ($r^2 = 0.19$, 0.25 and 0.19, respectively). However, there was no significant relationship between %HNA , LNA cell abundances or HNA cell abundances with temperature in the "surface" layers where the temperature range was the highest.

3.4 Patterns in cytometric parameters

Standardized SSC of HNA and LNA cells ranged from 0.0093 to 0.0265 and from 0.078 to 0.0185, respectively. Standardized green fluorescence of HNA and LNA cells ranged from 0.18 to 0.44 and from 0.050 to 0.097, respectively. The coefficient of variation of SSC was slightly higher for HNA cells (21 %) than for LNA cells (17 %). This was the same for green fluorescence (15 % versus 12 %).

Green fluorescence of LNA cells decreased slightly with depth (log–log regressions, $r^2 = 0.24$, $n = 493$, Fig. 4e and Fig. 5 e,f). In marked contrast, the green fluorescence of the HNA cells increased significantly with depth ($r^2 = 0.51$, data Fig. 4f and Fig. 5e, f) and with nutrients ($r^2 = 0.45$ for phosphate, $r^2 = 0.56$ for nitrate + nitrite, relation not shown).

The ANOVA analysis of SSC and green fluorescence based on the "chlorophyll"-defined depth layers suggests that this discrimination criterion was particularly appropriate in explaining the variability in green fluorescence of HNA cells ($n = 489$, $F = 356$), and to a lesser degree of LNA cells ($F = 32$, Fig. 4e, f). This discrimination criterion was more or less able to explain variability in SSC of the two groups ($F = 90$ for LNA cells, $F = 76$ for HNA cells, Fig. 4c, d).

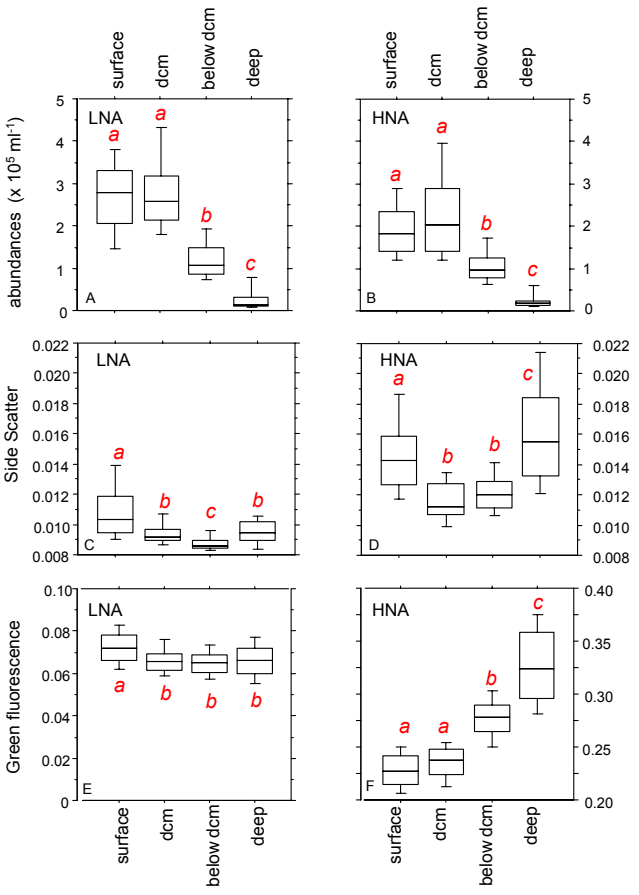

Fig. 4. Box plots showing distribution of (**A, B**): abundances, **(C, D)**: side scatter and **(E, F)**: green fluorescence of subgroups LNA and HNA along different water column layers: above the deep chlorophyll maximum ("surface"), at the deep chlorophyll maximum ("dcm"), below the dcm but above or equal to 250 m ("below dcm"), and below 250 m ("deep"). Groups connected by the same letter (in italics and in red) are not significantly different at the 0.01 probability level. Lower to the upper values are indicated, respectively, 10 %, 25 %, 50 % (median), 75 and 90 % percentiles.

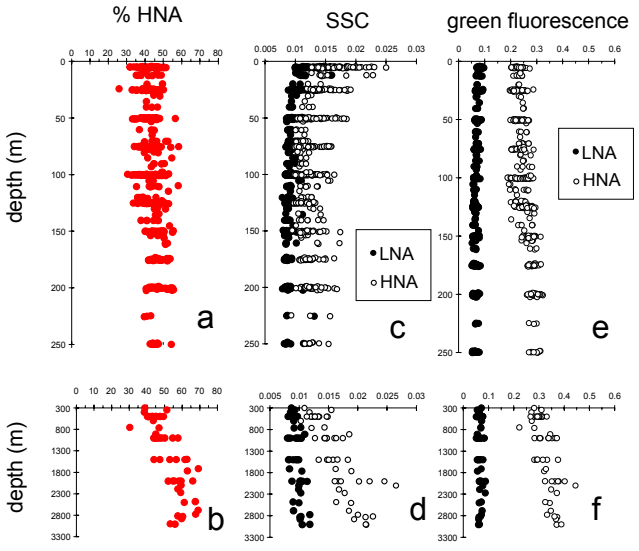

Fig. 5. Vertical distributions of **(a, b)**: percentage of HNA cells; **(c, d)**: side scatter signal (SSC); **(e, f)**: green fluorescence signal.

While green fluorescence characteristics were very distinct between the HNA and LNA cells regardless of depth, SSC differences were slight within surface layers but surprisingly higher in meso and bathy pelagic layers (Fig. 5d and Fig. 4d). SSC decreased with depth in "surface" layers (log–log regressions, model I, $p < 0.001$, $r^2 = 0.37$ for HNA cells $p < 0.001$, $r^2 = 0.46$ for LNA cells, Fig. 5c). In contrast, SSC increased in "deep" layers ($p < 0.001$, $r^2 = 0.66$ for HNA cells, $p < 0.001$, $r^2 = 0.27$ for LNA cells. This was more pronounced for HNA cells. Indeed, SSC of this group increased 6 times more rapidly with depth than the SSC of the LNA cells (Fig. 5d). The cytometric properties (SSC, fluorescence) of HNA and LNA cells showed low or inexistent relationships with nutrient concentrations when the depth effect was removed (i.e. when looking for relationships with NO_3^- + NO_2^- or PO_4^{3-} inside the different chlorophyll layers). Within "surface" layer, regional effects on SSC was inexistent for LNA (Fig. 6c) or scarce for HNA (Fig. 6d). Green fluorescence of both cytometric groups slightly decreased toward East ("St" and "Ea" regions for LNA, "Ea" region for HNA, Fig. 6e, f).

4 Discussion

4.1 Links with resources: chlorophyll and nutrient availability

In a given bacterioplankton population, HNA cells have been considered as the very active and dynamic cytometrically-defined group with high cell-specific activity rates (Servais et al., 1999; Lebaron et al., 2001; Longnecker et al., 2005, 2006). Therefore, the percentage of HNA cells relative to total abundance (%HNA) is generally related to variables tracking the productivity index of the ecosystem, such as chlorophyll stocks or bacterial production (Corzo et al., 2005; Moran et al., 2007). In our study, the percentage of HNA decreased slightly, but significantly, with increasing BP. It showed also very weak negative correlation with TChl-*a*. This is in contrast with what has been reported for large scale productivity gradients for which the correlation between %HNA and chlorophyll is generally positive (Bouvier et al., 2007 with a Chl-*a* gradient from 0.1 to 69 $\mu g\,l^{-1}$, Sherr et al., 2006 with a Chl-*a* gradient from 0.2 to 20 $\mu g\,l^{-1}$). For gradients much closer to our context, the reported correlations are much more variable, sometimes positive (Moran and Calvo-Diaz, 2009), negative (Nishimura et al., 2005) or even showing no significant correlation (Corzo et al., 2005).

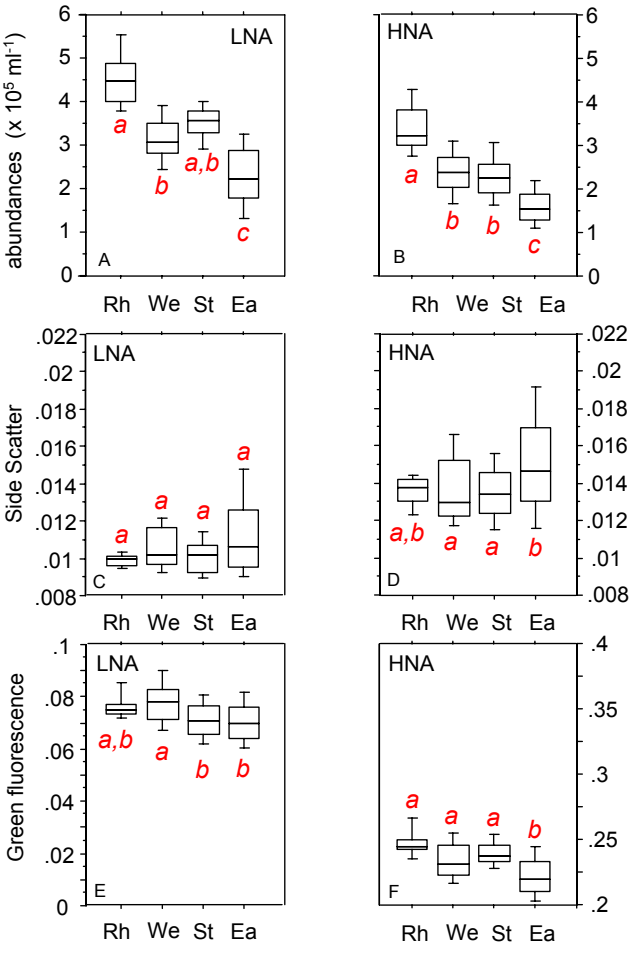

Fig. 6. Box plots showing distribution of (**A, B**): abundances, (**C, D**): side scatter and (**E, F**): green fluorescence of subgroups LNA and HNA in the "surface" layers according a regional distribution: "Rh" (stations 27, 26, 25), "We" (stations 24, 23, A, 22, 21, 20, 19), "St" (Stations 18, 17, 16, 15, 14) and "Ea" (stations 13, 12, B, 1, 2, 3, 4, 5, 6, 7, 8, 9, 10, C). Groups connected by the same letter (in italics and in red) are not significantly different at the 0.01 probability level.

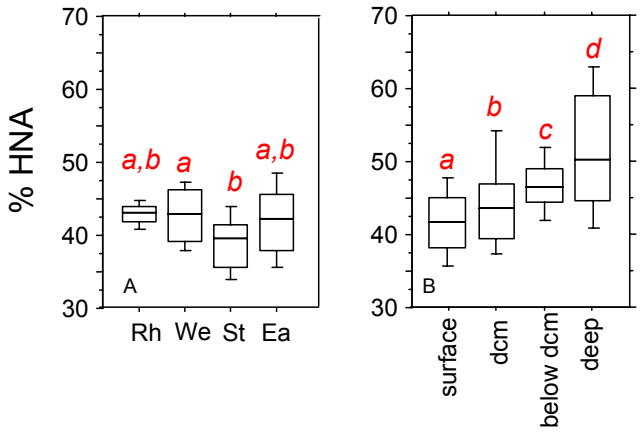

Fig. 7. Box plots showing distributions of %HNA in the different regions for the surface layers **(A)** and distribution of %HNA in the different layers (all stations included, **(B)**). Within a common layer, groups connected by the same letter (in italics and in red) are not significantly different at the 0.01 probability level.

These very contrasting results suggest that the bulk activity is not only controlled by HNA cells since some active cells may be spread differentially across distinct groups of bacterioplankton or that other environmental variables are better predictors of the relative importance of HNA cells.

In the stratified Mediterranean Sea, the dynamics of heterotrophic bacterial communities in surface layers is linked to the availability of inorganic resources, mostly P alone, sometimes N + P and in few occasions, N alone (Sala et al., 2002; Van Wambeke et al., 2002). Consequently, we also examined the relationships between inorganic nutrient concentrations and the %HNA. The %HNA was slightly more strongly correlated with PO_4^{3-} or NO_3^- + NO_2^- concentrations ($r^2 = 0.21$ and 0.23, respectively) than with TChl-*a* ($r^2 = 0.07$). As the vertical variability of nutrient concentration is important, the longitudinal effect could only be studied by comparing different layers. However, although mean nutrient concentrations showed a few statistical differences between some regions (mainly between "Ea" and "We"), we could not find any distinct patterns of %HNA longitudinally among the different regions compared. This idea is reinforced by the fact that the %HNA was not related to PO_4^{3-} or NO_3^- + NO_2^- concentration when considering layers independently. This suggests that HNA and LNA distributions are much more affected by the vertical stratification than by the longitudinal distribution. During the BOUM cruise, the effects of inorganic nutrient additions was examined in microcosm experiments in the three gyre stations using surface layer waters (Tanaka et al., 2011). In the surface samples (8 m depth), BP was stimulated by N (station B) or N + P (station C, Tanaka et al., 2011). Nishimura et al. (2005) hypothesized that P limitation exerts more severe constraints on the growth of bacterial groups with higher nucleic acid content. However at station B, N addition resulted in a 2 fold increase of cell specific activity of all cytometric groups, including LNA, HNA with low SSC and HNA with high SSC (Talarmin et al., 2011). Thus, it appeared that all cytometric groups reacted on the same way to nutrient additions, suggesting that both HNA and LNA cells were nutrient limited. This could explain why the %HNA in "surface" layers did not change in the more oligotrophic conditions in the East (Fig. 7a).

Both temperature and nutrient limitation could play a role in the distribution of cytometric groups. Indeed, referring to a modelling study by Hall et al. (2008), warm-adapted species could have lower minimal P cell quotas than cold-adapted species. This would confer an advantage to cells having low nucleic acid content (as nucleic acids are an important

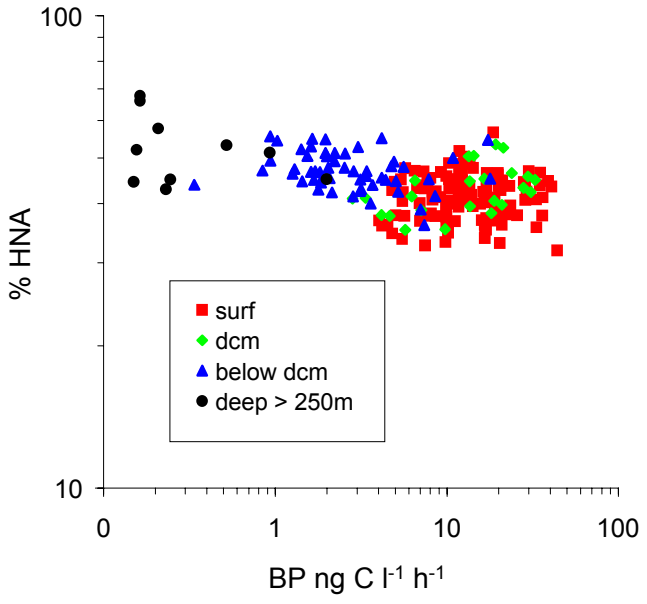

Fig. 8. Relationships between bacterial production and the percentage of HNA cells.

intracellular source of P) in warm, resource-limited environment. But the temperature role could be discounted as the temperature range in the "surface" layers during our study was great (around 11 °C: 26 °C down to 15 °C) and across this range the %HNA was not related to the temperature.

The cytometric properties of HNA and LNA cells were affected differently below the "surface" layers. Size scatter of HNA cells decreases, and green fluorescence of HNA cells increases (whereas that of LNA decreased). Interestingly, Talarmin et al. (2011) showed, through ^{3}H leucine labelling coupled to cell sorting, that the contribution of LNA cells to bulk leucine incorporation rates was higher in surface waters whereas that of HNA cells was higher at the vicinity of the dcm at the three sites A, B and C. This is in accordance with the positive and significant relationship between BP and %HNA at the dcm (Table 2). Possible explanations for these trends are a switch from nutrient to carbon limitation which is generally observed within the dcm in stratified conditions (Sala et al., 2002; Van Wambeke et al., 2002). This is associated with large changes in taxonomic composition of heterotrophic prokaryotes (Ghiglione et al., 2008; Van Wambeke et al., 2009). Apparently the HNA group benefits more of such changes than the LNA. This suggests, possibly, HNA group as a better driver of production when C is the resource limiting BP.

4.2 Deep layers

The relationships between the cytometric parameters of HNA and LNA cells were examined throughout the water column. One striking feature was the increase in the percentage of HNA with depth in the meso and bathypelagic zones ($r^2 = 0.59$, $n = 55$, $p < 0.001$). Since both abundances of HNA and LNA cells decreased with depth, this increase in %HNA was due to the 2 times larger decrease in LNA cell abundances with depth than that of HNA cells. This increase of %HNA is accordance with other reports. In the Atlantic, the %HNA has been shown to increase from 60 to 70 % at some stations between 600–750 m and 1000 m depth (Gasol et al., 2009). In the deep North Atlantic (down to 3800 m), Reinthaler et al. (2006) also reported an increase in the %HNA with depth but the data were not shown. Variations in HNA and LNA groups with depth were shown to occur following de-stratification of the water column (Winter et al., 2009). Another interesting and original feature from our study was the systematic increase in SSC and green fluorescence values of HNA cells with depth in the meso and bathypelagic zones (Fig. 5). SSC of LNA cells also increased with depth but 6 times less than that of HNA cells. SSC values of both HNA and LNA cells were not correlated to BP in the deep layers, nor to nutrient (PO_4^{3-}, NO_3^- + NO_2^-) concentrations. Since SSC variations are sometimes related to biovolume (Bouvier et al., 2001; Felip et al., 2007) the SSC increase could be interpreted as an increase in cell biovolume but this should be considered with caution. La Ferla et al. (2004) investigated the biovolume and lipopolysaccharide content of bacterioplankton down to 4000 m in the Ionian Sea and the mean cell volume varied in a similar range in both the euphotic and aphotic zone. It is important to consider that SSC isa complex variable not only and directly related to cell biovolume but also depends on the cell structure and the chemical composition of the outer membranes. The reasons underlying the increase in the %HNA and SSC of both HNA and LNA in deep layers are not clearly known. They may be related (i) to membrane properties changes due to hydrostatic pressure, (ii) to a switch from Eubacteria to Archaea dominance and, (iii) to differential aspects of predation and/or viral lysis on HNA and LNA cells (Wilson et al., 2001; Corzo et al., 2005; Tamburini et al., 2009; Winter et al., 2009).

5 Conclusions

To the best of our knowledge, this is the first investigation of the cytometric properties of HNA and LNA cells over large depth scales and longitudinal gradients in the oligotrophic Mediterranean Sea. Although the proportions of the HNA and LNA cells did not vary a lot, their cytometric characteristics showed distinct properties and relationships with other environmental variables in distinct chlorophyll- defined depth layers, and this might be related to the switch from nutrient to carbon limitation. %HNA and SSC of HNA cells are distinctly higher in the bathypelagic layers, suggesting that the activity in the two groups and/or environmental controls on HNA and LNA cells differ vertically. In contrast, cytometric properties and %HNA varied little with longitude

across the large transect sampled. Further investigations will be needed to understand these trends among these cytometric groups. There is more and more evidence suggesting that different groups are not only related to different specific activities but probably also phyologenetically, perhaps with some specific groups detected as HNA or LNA cells independent of their physiological state. The combination of tools such as cell sorting with activity measurements, subsequent cloning/sequencing (Guillebault et al., 2010), and investigation of individual cell C/N/P quotas (Twining et al., 2008) will be essential to better understand the ecological meaning of the ubiquitous presence of LNA and HNA cells in aquatic environments.

Acknowledgements. This research was founded by the French INSU-CNRS and by the SESAME project (Southern European Seas: Assessing and Modelling Ecosystem Changes), EC Contract No GOCE-036949, funded by the European Commission's Sixth Framework Programme. The authors would like to thank Thierry Moutin for leadership of the project and chief scientist of the BOUM cruise, Stella Psarra and Joséphine Ras for total chlorophyll sampling and analysis, Claude Courties and Christian Tamburini for discussions, John Dolan for improvement of the English and anonymous reviewers for their helpful comments in the first version of this ms.

Edited by: C. Jeanthon

The publication of this article is financed by CNRS-INSU.

References

Billen, G., Servais, P., and Becquevort, S.: Dynamics of bacterioplankton in oligotrophic and eutrophic aquatic environments: bottom-up or top-down control? Hydrobiologia, 27, 37–42, 1990.

Bouvier, T., Troussellier, M., Anzil, A., Courties, C., and Servais, P.: Using light scatter signal to estimate biovolume by flow cytometry, Cytometry, 44, 188–194, 2001.

Bouvier, T., Del Giorgio, P., and Gasol, J.: A comparative study of the cytometric characteristics of high and low nucleic acid bacteriaoplankton cells from different aquatic ecosystems, Environ. Microbiol., 9, 2050–2066, 2007.

Corzo, A., Rodríguez-Gálvez, S., Lubian, L., Sobrino, C., Sangrá, P., and Martínez, A.: Antarctic marine bacterioplankton subpopulations discriminated by their apparent content of nucleic acids differ in their response to ecological factors, Polar Biol., 29, 27–39, 2005.

Crombet, Y., Leblanc, K., Quéguiner, B., Moutin, T., Rimmelin, P., Ras, J., Claustre, H., Leblond, N., Oriol, L., and Pujo-Pay, M.: Deep silicon maxima in the stratified oligotrophic Mediterranean Sea, Biogeosciences, 8, 459–475, doi:10.5194/bg-8-459-2011, 2011.

Ducklow, H. W.: Factors regulating bottom-up control of bacterial biomass in open ocean plankton communities, Arch. Hydrobiol. Beih. Ergebn. Limnol., 37, 207–217, 1992.

Felip, M., Andreatta, S., Sommaruga, R., Straskrabova, V., and Catalan, J.: Suitability of flow cytometry for estimating bacterial biovolume in natural plankton samples: comparison with microscopy data, Appl. Environ. Microbiol., 73, 4508–4514, 2007.

Gasol, J. M., Alonso-Saez, L., Vaqué, D., Baltar, F., Calleja, M., Duarte, C. M., and Aristegui, J.: Mesopelagic prokaryotic bulk and single cell heterotrophic activity and community composition in the NW Africa – Canary Islands coastal-transition zone, Prog. Oceanogr., 83, 189–196, 2009.

Ghiglione, J. F., Palacios, C., Marty, J. C., Mével, G., Labrune, C., Conan, P., Pujo-Pay, M., Garcia, N., and Goutx, M.: Role of environmental factors for the vertical distribution (0-1000 m) of marine bacterial communities in the NW Mediterranean Sea, Biogeosciences, 5, 1751–1764, doi:10.5194/bg-5-1751-2008, 2008.

Guillebault, D., Laghdass, M., Catala, P., Obernosterer, I., and Lebaron, P.: Improved Method for Bacterial Cell Capture after Flow Cytometry Cell Sorting, Appl. Environ. Microbiol, 76, 7352–7355, 2010.

Hall, E. K., Neuhauser, C., and Cotner, J.: toward a mechanistic understanding of how natural bacterial communities respond to changes in teperature in aquatic ecosystems, The ISME Journal, 2, 471–481, 2008.

Joux, F., Servais, P., Naudin, J.-J., Lebaron, P., Oriol, L., and Courties, C.: Distribution of picophytoplankton and bacterioplankton along a river plume gradient in the Mediterranean Sea, Vie et Milieu, 55, 197–208, 2005.

Kirchman, D. L.: Leucine incorporation as a measure of biomass production by heterotrophic bacteria, in: Handbook of methods in aquatic microbial ecology, edited by: Kemp, P. F., Sherr, B. F., Sherr, E. B., and Cole, J. J., Lewis, 509–512, 1993.

La Ferla, R., Giudice, A., and Maimone, G.: Morphology and LPS content for the estimation of marine bacterioplankton biomass in the Ionian Sea, Sci. Mar., 68, 23–31, 2004.

Lebaron, P., Servais, P., Agogué, H., Courties, C., and Joux, F.: Does the High Nucleic Acid Content of Individual Bacterial Cells Allow Us To Discriminate between Active Cells and Inactive Cells in Aquatic Systems?, Appl. Environ. Microbiol., 67, 1775–1782, 2001.

Li, W. K. W., Jellet, J. F., and Dickie, P. M.: DNA distributions in planktonic bacteria stained with TOTO or TO-PRO, Limnol. Oceanogr., 40, 1485–1495, 1995.

Longnecker, K., Sherr, B. F., and Sherr, E. B.: Activity and phylogenetic diversity of bacterial cells with high and low nucleic acid content and electron transport system activity in an upwelling ecosystem, Appl. Environ. Microbiol., 71, 7737–7749, 2005.

Longnecker, K., Sherr, B. F., and Sherr, E. B.: Variation in cell specific rates of leucine and thymidine incorporation by marine bacteria with high and low nucleic acid content off the Oregon coast, Aquat. Microb. Ecol., 43, 113–125, 2006.

Mével, G., Vernet, M., Goutx, M., and Ghiglione, J. F.: Seasonal to hour variation scales in abundance and production of total and particle-attached bacteria in the open NW Mediterranean Sea

(0-1000 m), Biogeosciences, 5, 1573–1586, doi:10.5194/bg-5-1573-2008, 2008.

Moran, X. A. and Calvo-Diaz, A.: Single cell vs bulk activity properties of coastal bacterioplankton over an annual cycle in a temperate ecosystem, FEMS Microb. Ecol., 67, 43–56, 2009.

Moran, X. A., Bode, A., Suarez, L. A., and Nogueira, E.: Assessing the relevance of nucleic acid content as an indicator of marine bacterial activity, Aquat. Microb. Ecol, 46, 141–152, 2007.

Moran, X. A., Calvo-Diaz, A., and Ducklow, H. W.: Total and phytoplankton mediated bottom-up control of bacterioplankton change with temperature in the NE Atlantic shelf waters, Aquat. Microb. Ecol., 58, 229–239, 2010.

Moutin, T., Van Wambeke, F., and Prieur, L.: Introduction to the Biogeochemistry from the Oligotrophic to the Ultraoligotrophic Mediterranean experiment: the BOUM program, Biogeosciences Discuss., in prep., 2011.

Nishimura, Y., Kim, C., and Nagata, T.: Vertical and seasonal variations of bacterioplankton subgroups with different nucleic acid contents: possible regulation by phosphorus, Appl. Environ. Microbiol., 71, 5828–5836, 2005.

Pujo-Pay, M., Conan, P., Oriol, L., Cornet-Barthaux, V., Falco, C., Ghiglione, J.-F., Goyet, C., Moutin, T., and Prieur, L.: Integrated survey of elemental stoichiometry (C, N, P) from the western to eastern Mediterranean Sea, Biogeosciences, 8, 883–899, doi:10.5194/bg-8-883-2011, 2011.

Ras, J., Claustre, H., and Uitz, J.: Spatial variability of phytoplankton pigment distributions in the Subtropical South Pacific Ocean: comparison between in situ and predicted data, Biogeosciences, 5, 353–369, doi:10.5194/bg-5-353-2008, 2008.

Reinthaler, T., Van Aken, H., Veth, C., Aristegui, C., Robinson, C., Williams, P. J. le B., Lebaron, P., and Herndl, G.: Prokaryotic respiration and production in the meso and bathypelagic realm of the Eastern and Western North Atlantic Basin, Limnol. Oceanogr., 51, 1262–1273, 2006.

Sala, M. M., Peters, F., Gasol, J. M., Pedros-Alio, C., Marrasse, C., and Vaque, D.: Seasonal and spatial variations in the nutrient limitation of bacterioplankton growth in the Northwestern Mediterranean, Aquat. Microb. Ecol., 27, 47–56, 2002.

Scharek, R. and Latasa, M.: Growth, grazing and carbon flux of high and low nucleic acid bacteria differ in surface and deep chlorophyll maximum layers in the NW Mediterranean Sea, Aquat. Microb. Ecol., 46, 153–161, 2007.

Schlitzer, R.: Ocean Data View 4, http://odv.awi.de, 2009.

Servais, P., Courties, C., Lebaron, P., and Trousselier, M.: Coupling bacterial activity measurements with cell sorting by flow cytometry, Microb. Ecol., 38, 180–189, 1999.

Sherr, B., Sherr, E., and Longnecker, K.: distribution of bacterial abundance and cell-specific nucleic acid content in the Northeast Pacific Ocean, Deep-Sea Res. Pt. I, 53, 713–725, 2006.

Smith, D. C. and Azam, F.: A simple, economical method for measuring bacterial protein synthesis rates in sea water using 3H-Leucine, Mar. Microb. Food Webs, 6, 107–114, 1992.

Sokal, R. R. and Rohlf, F. J.: Biometry, 2 Edn., edited by: Freeman W. H. and Company, New York, 1981.

Talarmin, A., Van Wambeke, F., Catala, P., Courties, C., and Lebaron, P.: Flow cytometric assessment of specific leucine incorporation in the open Mediterranean, Biogeosciences, 8, 253–265, doi:10.5194/bg-8-253-2011, 2011.

Tanaka, T., Thingstad, T. F., Christaki, U., Colombet, J., Cornet-Barthaux, V., Courties, C., Grattepanche, J.-D., Lagaria, A., Nedoma, J., Oriol, L., Psarra, S., Pujo-Pay, M., and Van Wambeke, F.: Lack of P-limitation of phytoplankton and heterotrophic prokaryotes in surface waters of three anticyclonic eddies in the stratified Mediterranean Sea, Biogeosciences, 8, 525–538, doi:10.5194/bg-8-525-2011, 2011.

Tamburini, C., Garel, M., Al Ali, B., Mérigot, B., Kriwy, P., Charrière, B., and Budillon, G.: Distribution and activity of Bacteria and Archaea in the different water masses of the Tyrrhenian Sea, Deep Sea Res. Pt. II, 56, 700–712, 2009.

Twining, B. S., Baines, S., Vogt, S., and de Jonge, M. D.: Exploring ocean biogeochemistry by single cell microprobe analysis of protist elemental composition, J. Eukaryot. Microbiol., 55, 151–162, 2008.

Van Wambeke, F., Christaki, U., Giannakourou, A., Moutin, T., and Souvemerzoglou, K.: Longitudinal and vertical trends of bacterial limitation by phosphorus and carbon in the Mediterranean Sea, Microb. Ecol., 43, 119–133, 2002.

Van Wambeke, F., Ghiglione, J.-F., Nedoma, J., Mével, G., and Raimbault, P.: Bottom up effects on bacterioplankton growth and composition during summer-autumn transition in the open NW Mediterranean Sea, Biogeosciences, 6, 705–720, doi:10.5194/bg-6-705-2009, 2009.

Wilson, W. W., Wade, M. M., Holman, S. C., and Champlin, F. R.: Status of methods for assessing bacterial cell surface charge properties based on zeta potential measurements, J. Microbiol. Meth., 43, 153–164, 2001.

Winter, C., Kerros, M.-E., K., and Weinbauer, M.: Seasonal and depth-related dynamics of prokaryotes and viruses in surface and deep waters of the Northwestern Mediterranean Sea, Deep Sea Res. Pt. I, 56, 1972–1982, 2009.